

# Relevance Subject Machine: A Novel Person Re-identification Framework

Igor Fedorov, *Student Member, IEEE*, Ritwik Giri, *Student Member, IEEE*, Bhaskar D. Rao, *Fellow, IEEE*,  
Truong Q. Nguyen, *Fellow, IEEE*

**Abstract**—We propose a novel method called the Relevance Subject Machine (RSM) to solve the person re-identification (re-id) problem. RSM falls under the category of Bayesian sparse recovery algorithms and uses the sparse representation of the input video under a pre-defined dictionary to identify the subject in the video. Our approach focuses on the multi-shot re-id problem, which is the prevalent problem in many video analytics applications. RSM captures the essence of the multi-shot re-id problem by constraining the support of the sparse codes for each input video frame to be the same. Our proposed approach is also robust enough to deal with time varying outliers and occlusions by introducing a sparse, non-stationary noise term in the model error. We provide a novel Variational Bayesian based inference procedure along with an intuitive interpretation of the proposed update rules. We evaluate our approach over several commonly used re-id datasets and show superior performance over current state-of-the-art algorithms. Specifically, for ILIDS-VID, a recent large scale re-id dataset, RSM shows significant improvement over all published approaches, achieving an 11.5% (absolute) improvement in rank 1 accuracy over the closest competing algorithm considered.

**Index Terms**—Re-identification, sparse coding, sparse Bayesian learning

## 1 INTRODUCTION

CAMERA networks have become increasingly commonplace in crowded public settings, such as airports and subways. These networks can be used as a tool for improving public safety by enabling the identification and tracking of target individuals [1]. We focus on the person re-identification (re-id) task, which refers to determining the identity of an individual in a video given a database of camera footage [2]. The input video is often referred to as the probe and the database as the gallery [3]. The gallery may consist of videos recorded from the same camera as the probe video or from different cameras [4]. The re-id problem is challenging because subjects may be occluded in the probe and/or gallery, and there may be significant illumination and perspective variation between the gallery and probe.

The defining characteristics of re-id algorithms are the representation of video frames (the feature space) and the method by which the probe is matched to the subjects in the gallery (the ranking system). There is already a significant body of work in defining highly robust and discriminative feature spaces for the re-id task [5], [6], [7], [8], [9], [10], [11], [12], [13], [14], [15], [16], [17], [18], [19]. In addition, much work has been done in studying ranking schemes for the case when the probe contains a single frame [7], [10], [20], [21], [22]. In many instances, researchers extend their ranking algorithms to the scenario where the probe contains *multiple* frames [3], [7] without exploiting a significant amount of information provided by the *collection* of probe frames. The primary motivation for our work is to develop a ranking scheme specifically tailored for the multi-shot re-id problem. As such, we focus primarily on the design of the ranking strategy, assuming that the feature space has been pre-defined.

### 1.1 Problem Formulation

Let  $\{\mathbf{A}_{(:,i)} \in \mathbb{R}^d\}_{i=1}^N$  represent the set of gallery frames, in a pre-defined feature space, as shown in Fig. 1. Note that each  $\mathbf{A}_{(:,i)}$  is associated with a subject labeled with index  $\mathbf{s}_i$ ,  $1 \leq \mathbf{s}_i \leq C$ , where  $C$  is the total number of subjects. Let  $\{\mathbf{Y}_{(:,i)} \in \mathbb{R}^d\}_{i=1}^L$  represent the set of frames for a given probe. The goal of re-id is to generate  $\boldsymbol{\Psi} \in \mathbb{R}^C$ , where  $\boldsymbol{\Psi}_r$  is the rank  $r$  estimate of the identity of the subject in the probe.

The re-id problem has two distinct variants: single or multi-shot [10]. The number of probe frames  $L$  is constrained to be 1 for single-shot, whereas  $L > 1$  for multi-shot. In both cases, the gallery  $\mathbf{A}$  may contain one or more columns corresponding to each subject.

Recently, sparsity based methods have become increasingly popular in computer vision contexts [20], [23], including re-id [3], [7], [24]. Specifically, the sparse representation-based classification (SRC) [20] framework has become a common-place building block in numerous applications. In the context of re-id, SRC can be seen as a way of addressing the single-shot problem. The idea is to first solve the following sparse recovery (SR) problem

$$\arg \min_{\mathbf{x}} \underbrace{\|\mathbf{y} - \mathbf{A}\mathbf{x}\|_2^2}_{\text{Modeling error}} + \underbrace{\lambda \|\mathbf{x}\|_1}_{\text{Sparsity regularizer}}, \quad (1)$$

where we use  $\mathbf{y}$  to denote  $\mathbf{Y}_{(:,1)}$  for brevity. We refer to  $\mathbf{x}$  as the encoding of  $\mathbf{y}$  under  $\mathbf{A}$ . The  $\ell_1$  regularizer in (1) promotes sparse  $\mathbf{x}$  [25], [26], i.e.  $\mathbf{x}$  that has many zeros. The hypothesis is that  $\mathbf{y}$  lies in a subspace spanned by  $\{\mathbf{A}_{(:,i)}\}_{i:\mathbf{s}_i=c^*}$ , where  $c^*$  is the identity of the subject in  $\mathbf{y}$ . Under this hypothesis, the support of  $\mathbf{x}$  can be treated as a good indicator of the identity of  $\mathbf{y}$ . To generate  $\boldsymbol{\Psi}$ , the residuals

$$\mathbf{r}_c^{SRC} = \|\mathbf{y} - \mathbf{A}\boldsymbol{\phi}_c(\mathbf{x})\|_2 \quad (2)$$

*I. Fedorov, B.D. Rao and T.Q. Nguyen are with the Department of Electrical and Computer Engineering at the University of California, San-Diego. R. Giri was with the Department of Electrical and Computer Engineering at the University of California, San-Diego when the research for this work was conducted and is now with Starkey Hearing Technologies. I. Fedorov was partially supported by the San Diego Chapter of the ARCS Foundation, Inc.*

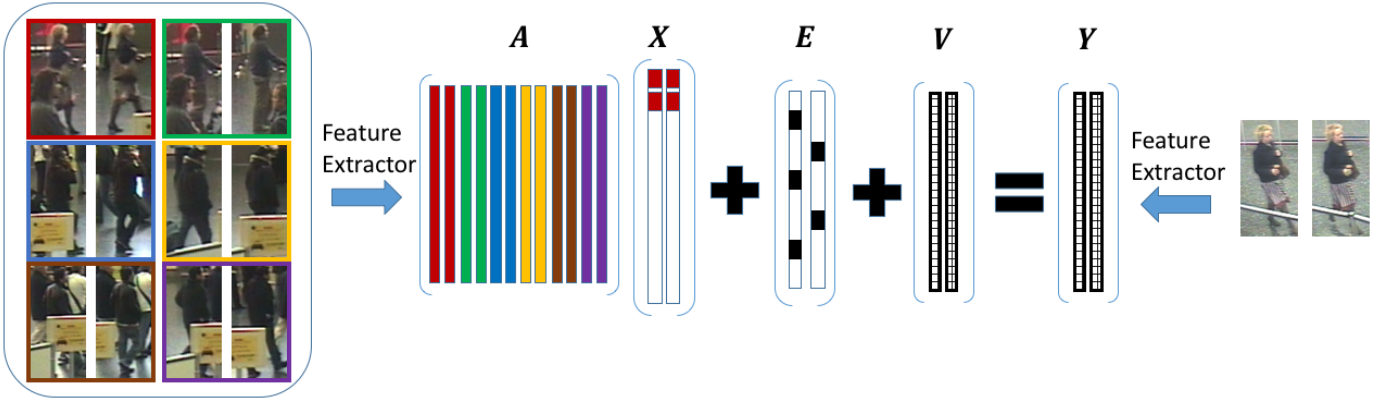


Fig. 1. Diagram of RSM signal model.

are first computed for all subjects  $c$ , where  $\phi_c(\cdot)$  is defined such that, if  $\mathbf{z} = \phi_c(\mathbf{x})$ , then

$$\mathbf{z}_j = \begin{cases} \mathbf{x}_j & \text{if } \mathbf{s}_j = c \\ 0 & \text{else.} \end{cases} \quad (3)$$

The elements of  $\mathbf{r}^{SRC}$  are then sorted in ascending order and  $\boldsymbol{\psi}$  is set to  $\boldsymbol{\rho}$ , where  $\mathbf{r}_{\rho_r}^{SRC}$  is the  $r$ 'th smallest element of  $\mathbf{r}^{SRC}$ .

While effective, the formulation in (1) is sub-optimal for the person re-id problem in many respects. One significant issue is that (1) ignores the inherent structure in  $\mathbf{A}$  when solving the SR problem. As Fig. 1 shows,  $\mathbf{A}$  has a *block* structure, where each block  $g_c = \{1 \leq i \leq N : \mathbf{s}_i = c\}$  corresponds to a specific subject in the gallery [3]. Given that  $\mathbf{A}$  has a block structure, (1) can be modified to solve a *block sparse recovery* problem [27], [28] by replacing the  $\ell_1$  regularizer with a block-sparsity regularizer.

Another issue with (1) is that it is sensitive to large outliers in the modeling error, which may occur because of occlusions, illumination changes, viewpoint variations, etc. To make the formulation more robust, the modeling error is often modified to include a dense (Gaussian) noise term *and* a sparse error term [20], represented by  $\mathbf{V}$  and  $\mathbf{E}$  in Fig. 1, respectively.

Most importantly, although (1) is a reasonable approach to the single-shot re-id problem, extending it to the multi-shot case is not straightforward. There have been several attempts at building upon the SRC framework for the multi-shot problem [3], [7]. The issue with these methods is that they neglect to exploit the fundamental advantage offered by the multi-shot re-id problem: The identity of the probe subject is constant for all probe frames  $\{\mathbf{Y}_{(:,i)}\}_{i=1}^L$ , meaning that  $\{\mathbf{X}_{(:,i)}\}_{i=1}^L$  should exhibit *joint* sparsity, i.e. the sparsity pattern of  $\mathbf{X}_{(:,i)}$  should be the same for all  $i$ , as shown in Fig. 1. Incorporating joint sparsity into the SR algorithm is known to produce superior results [29]. The lack of a re-id algorithm capable of exploiting joint sparsity motivates the present work.

## 1.2 Contribution

We propose a re-id framework which incorporates many of the advantages of previous SR based approaches, while also leveraging the information inherent in the multi-shot problem to a fuller extent.

- We employ a Bayesian approach to the SR problem, based on the Relevance Vector Machine (RVM) [30]. RVM has been shown to achieve much higher SR rates than many

deterministic approaches [31] and has the potential to outperform algorithms based on the formulation in (1) in the re-id task. We build upon the signal model we introduced in [32] and refer to our approach as the Relevance Subject Machine (RSM).

- Unlike [3], [7], RSM allows us to use all of the frames in the probe *within* the SR process and model the joint sparsity of  $\{\mathbf{X}_{(:,i)}\}_{i=1}^L$ . In addition, RSM allows us to model sparse, outlier noise prevalent in the re-id problem.
- We introduce a novel iterative candidate subject ranking strategy which leverages the superior SR performance of the Bayesian approach without making inference computationally intractable.
- We show that the proposed approach achieves state-of-the-art performance on multi-shot re-id datasets.

## 2 RELATED WORK

### 2.1 State-of-the-Art Sparse Re-Identification

SR based re-id algorithms are generally characterized by their representation of the video data, SR algorithm, and ranking scheme. A thorough review of popular feature spaces for the re-id problem can be found in [33]. Usually, a tracking algorithm is used to isolate a single subject in each frame. The remaining design choice is then to select the representation of the subject. Gray and Tao [8] split each frame into 6 horizontal strips, convolve each strip with 13 Schmid and 6 Gabor filters, and form a feature vector by quantizing the filter responses into 16 bin histograms. The feature vector is then appended with 16 bin histograms of the RGB, HSV, and YCbCr representations of each strip, resulting in a 2592-dimensional representation. Lisanti *et al.* [7] split each frame into overlapping horizontal stripes and extract RGB and Hue-Saturation histograms for each stripe, where the contribution of each pixel is weighted by an Epanechnikov kernel centered on the image. The feature vector is then appended with a Histogram of Oriented Gradient (HOG) descriptor computed over the entire frame, generating a 2960-dimensional representation referred to as the weighted histogram of overlapping stripes (WHOS). Liao *et al.* [13] describe the local maximal occurrence (LOMO) representation, where a 26960-dimensional representation is computed using a set of local horizontal features. Other feature spaces based on salience [15], symmetry driven accumulation of local features (SDALF) [10], and local binary patterns (LBP) [34] have been explored. In most cases, the number of features is *greater* than

the number of gallery frames. This motivates the approach in the present work, whose computational complexity is a function of the *minimum* of  $d$  and  $N$ .

In order to aid in classification, many approaches learn a projection (referred to as a metric) such that projected points from the same class are close to each other and far away from projected points from other classes [35]. Karanam *et al.* [3] use local Fisher discriminant analysis [36] to learn an embedding given training data for both the gallery and probe views. Liao *et al.* [13] present an efficient metric learning algorithm, called Cross-view Quadratic Discriminant Analysis (XQDA), aimed at learning projections when features are extracted from two separate views.

SR algorithms for re-id usually include solving a problem of the form given in (1). Khedher *et al.* [37] use (1) to extract sparse codes for each frame of a probe. Karanam *et al.* [3] propose the sparse re-id (SRID) framework where a block-sparse, outlier robust SR approach of the form

$$\begin{aligned} \underset{\mathbf{X}_{(:,i)}, \mathbf{E}_{(:,i)}}{\operatorname{argmin}} \quad & \|\mathbf{E}_{(:,i)}\|_1 + \sum_{c=1}^C \|\mathbf{X}_{(g_c,i)}\|_2 \\ \text{subject to} \quad & \mathbf{Y}_{(:,i)} = \mathbf{A}\mathbf{X}_{(:,i)} + \mathbf{E}_{(:,i)} \end{aligned} \quad (4)$$

is used for each probe frame  $i$ , where  $\mathbf{X}_{(g_c,i)}$  is shorthand for  $[\mathbf{X}_{(j_1,i)} \cdots \mathbf{X}_{(j_{|g_c|},i)}]^T$ ,  $j_k \in g_c$ . Lisanti *et al.* [7] propose an iterative sparse re-weighting (ISR) approach for the re-id problem where, at each iteration  $r$ , a problem of the form

$$\underset{\mathbf{X}_{(:,i)}}{\operatorname{argmin}} \|\mathbf{Y}_{(:,i)} - \mathbf{A}\mathbf{X}_{(:,i)}\|_2^2 + \lambda \|\mathbf{W}^r \mathbf{X}_{(:,i)}\|_1 \quad (5)$$

is solved for each probe frame  $i$ , where  $\mathbf{W}^r$  is a diagonal matrix whose  $(j,j)$ 'th entry is given by  $(\mathbf{X}_{(j,i)}^{r-1} + \varepsilon)^{-1}$ ,  $\varepsilon$  is a small positive constant, and  $\mathbf{X}_{(:,i)}^r$  denotes the estimate of  $\mathbf{X}_{(:,i)}$  at the  $r$ 'th iteration. The intuition for performing reweighting is to make the sparse-recovery algorithm robust against large non-zero values of  $\mathbf{X}_{(:,i)}$  [38], which heavily influence the  $\ell_1$  norm and can prevent formulations such as (1) from finding smaller valued coefficients that can be important for ranking. RSM incorporates the advantages of (4) and (5). Moreover, unlike previous SR based re-id approaches based on (1), (4), and (5) [3], [7], [24], [37], which solve the SR problem for each probe frame *independently*, we perform SR on the entire probe video under a joint sparsity assumption.

Ranking schemes used by SR based re-id algorithms usually take the form of computing a residual for each subject  $c$ , as in [3] where

$$\mathbf{r}_c^{SRID} = \sum_{i=1}^L \|\mathbf{Y}_{(:,i)} - \mathbf{E}_{(:,i)} - \mathbf{A}\phi_c(\mathbf{X}_{(:,i)})\|_2, \quad (6)$$

and sorting the result to produce  $\boldsymbol{\psi}$ . One variant of this approach is given in [7], where the residual computation is modified to

$$\mathbf{r}_c^{ISR} = \underset{i}{\operatorname{argmin}} \|\mathbf{Y}_{(:,i)} - \mathbf{A}\phi_c(\mathbf{X}_{(:,i)})\|_2 \quad (7)$$

and the ranking is generated iteratively. At each iteration  $r$ , a SR problem of the form (5) is solved for each probe frame  $i$ , the residuals in (7) computed, and  $\boldsymbol{\psi}_r$  set to  $\underset{c}{\operatorname{argmin}} \mathbf{r}_c^{ISR}$ . Before proceeding to the next iteration, columns corresponding to subject  $\boldsymbol{\psi}_r$  are removed from  $\mathbf{A}$  in order to prevent subjects which have already been ranked from influencing the ranking of the remaining subjects. We employ the residual definition in (6) because it encodes the reconstruction error for all  $L$  probe frames, which

is more aligned with our goal of *jointly* identifying  $\mathbf{Y}$ . In addition, we build upon the iterative ranking strategy in [7] in our RSM framework.

## 2.2 Bayesian Sparse Recovery

Recently, there has been much interest in Bayesian approaches for the SR problem. Tipping's seminal work [30] on the RVM offered a novel hierarchical Bayesian formulation for sparse regression and classification problems. Wipf and Rao [39] then adopted the RVM for the SR problem, showing that, in the noiseless setting, the local minima of the objective function being minimized are sparse and the global minimum is the *maximally sparse* encoding of  $\mathbf{y}$  under  $\mathbf{A}$ . Moreover, RVM has been shown to empirically outperform competing SR algorithms [31].

In the following, let  $\mathbf{y}$  and  $\mathbf{x}$  be vector random variables representing a single probe frame and its corresponding sparse code, respectively, under  $\mathbf{A}$ . The RVM signal model is given by

$$\mathbf{y} = \mathbf{A}\mathbf{x} + \mathbf{v} \quad (8)$$

where  $\mathbf{v} \sim N(0, \lambda \mathbf{I})$  represents signal noise. The sparse code  $\mathbf{x}$  is assigned a separable prior of the form  $p(\mathbf{x}) = \prod_{j=1}^N p(\mathbf{x}_j)$  where  $p(\mathbf{x}_j)$  has a Gaussian Scale Mixture (GSM) [40] representation given by

$$p(\mathbf{x}_j | \boldsymbol{\gamma}_j) = N(\mathbf{x}_j; 0, \boldsymbol{\gamma}_j). \quad (9)$$

The scale mixture representation is capable of representing most heavy-tailed densities [41], [42], [43], [44], [45], which are known to be suitable for promoting sparsity [29], [30]. The heavy-tailed nature of scale mixture priors allows us to model both the sparsity and large non-zero entries of  $\mathbf{x}$ . Note that the selection of  $p(\boldsymbol{\gamma})$  represents a choice of prior on  $\mathbf{x}$  [39]. The RVM framework seeks the maximizer  $\boldsymbol{\gamma}^*$  of the evidence  $p(\mathbf{y} | \boldsymbol{\gamma})$  and then estimates  $\mathbf{x}$  using the mode of  $p(\mathbf{x} | \mathbf{y}, \boldsymbol{\gamma}^*)$ .

One of the advantages of the RVM is that it is straightforward to encode prior knowledge about the recovery problem. For instance, if  $\mathbf{A}$  is known to be decomposable into disjoint blocks, the conditional density of  $\mathbf{x}$  given  $\boldsymbol{\gamma}$  is amended to [46]

$$p(\mathbf{x} | \boldsymbol{\gamma}) = \prod_{c=1}^C \prod_{j \in g_c} N(\mathbf{x}_j; 0, \boldsymbol{\gamma}_c) \quad (10)$$

and the inference procedure remains the same. Note that, whereas  $\boldsymbol{\gamma} \in \mathbb{R}^N$  in (9),  $\boldsymbol{\gamma} \in \mathbb{R}^C$  in (10). To additionally encode joint sparsity among the columns of  $\mathbf{X}$ , we can define a *matrix* conditional density of the form [29]

$$p(\mathbf{X} | \boldsymbol{\gamma}) = \prod_{c=1}^C \prod_{j \in g_c} N(\mathbf{X}_{(j,:)}; 0, \boldsymbol{\gamma}_c \mathbf{I}). \quad (11)$$

Joint sparsity is enforced in (11) by the fact that  $\boldsymbol{\gamma}_c$  is shared for all  $j \in g_c$  among all  $\{\mathbf{X}_{(j,:)}\}_{i=1}^L$ . Finally, incorporating robustness to sparse noise is achieved by modifying (8) to [47]

$$\mathbf{y} = \mathbf{A}\mathbf{x} + \mathbf{v} + \mathbf{e} \quad (12)$$

where  $\mathbf{e}$  is itself assigned a separable GSM prior to promote sparsity.

The combination of block sparsity, robustness to sparse noise, and joint sparsity over multiple observations was first studied by us in [32]. The signal model considered was

$$\mathbf{Y} = \mathbf{A}\mathbf{X} + \mathbf{V} + \mathbf{E}, \quad (13)$$

where  $p(\mathbf{X}|\boldsymbol{\gamma})$  is given by (11) and  $p(\mathbf{E}|\mathbf{D})$  is given by

$$p(\mathbf{E}|\mathbf{D}) = \prod_{j=1}^d \prod_{i=1}^L N(\mathbf{E}_{(j,i)}; \mathbf{0}, \mathbf{D}_{(j,i)}). \quad (14)$$

Although the joint block sparsity constraint is a valid one for the encoding matrix  $\mathbf{X}$ , it does not hold for the outlier matrix  $\mathbf{E}$  since the outliers can be time varying. Because the Inverse Gamma ( $IG$ ) distribution is the conjugate prior for the variance of a Gaussian likelihood, we specify  $p(\boldsymbol{\gamma}_c) = IG(\alpha_\gamma, \beta_\gamma)$  and  $p(\mathbf{D}_{(j,i)}) = IG(\alpha_\delta, \beta_\delta)$ .

To the best of our knowledge, we are the first to apply the RVM framework to person re-id. One reason why previous researchers may have been reluctant to apply the RVM to re-id may be that inference was computationally intractable. To combat this, we propose a ranking strategy based on [7] which can be readily used within our RSM framework without adding a significant amount of additional computation. Finally, we apply metric learning to reduce the dimensionality of the problem, where appropriate.

### 3 APPROACH

In this section, we describe the inference and ranking strategies in detail. We begin by introducing Variational Bayesian (VB) inference in Section 3.1. We show the VB inference procedure for RSM in Section 3.2 and the ranking strategy in Section 3.3.

#### 3.1 Variational Bayesian Inference Background

Let  $\mathbf{z}$  and  $\mathbf{y}$  denote the set of all latent and observed variables, respectively, in a given model. To estimate the set of desired parameters, which are included in  $\mathbf{z}$ , the goal is to find the posterior density  $p(\mathbf{z}|\mathbf{y})$ . The primary hindrance to computing this posterior lies in the integration required to find the normalizing factor  $p(\mathbf{y}) = \int p(\mathbf{y}|\mathbf{z})p(\mathbf{z})d\mathbf{z}$ , which makes computing  $p(\mathbf{z}|\mathbf{y})$  intractable for most densities of interest. In VB [48], [49], [50], this problem can be bypassed by approximating  $p(\mathbf{z}|\mathbf{y})$  by a factorized distribution  $q(\mathbf{z}) = \prod_{k=1}^K q_k(\mathbf{z}_k)$  where  $\mathbf{z}_k$  denotes a subset of  $\mathbf{z}$ . Consider the log marginal probability of  $\mathbf{y}$

$$\log p(\mathbf{y}) = L(q(\mathbf{z})) + KL(q(\mathbf{z}) || p(\mathbf{z}|\mathbf{y})), \quad (15)$$

where the first term is defined as

$$L(q) = \int q(\mathbf{z}|\mathbf{y}) \log \frac{p(\mathbf{y}, \mathbf{z})}{q(\mathbf{z}|\mathbf{y})} d\mathbf{z} \quad (16)$$

and can be interpreted as the lower bound on the log marginal probability, while the second term is the Kullback-Leibler (KL) divergence between  $q$  and the true posterior. The aim is to maximize the lower bound with respect to  $q$ , which is equivalent to minimizing the KL divergence term.

Let us now select one subset  $\mathbf{z}_k$  and maximize  $L(q)$  with respect to  $q_k$ . It can be shown [48], [49], [50] that this optimization leads to the following update of  $q_k$ :

$$\log q_k = E_{k' \neq k} [\log p(\mathbf{y}, \mathbf{z})] \quad (17)$$

where  $E_{k' \neq k}[\dots]$  denotes an expectation with respect to  $q$  over all variables  $\mathbf{z}_{k'}$ ,  $k' \neq k$ . This procedure is then iteratively repeated for all subsets to convergence [51].

#### 3.2 Variational Bayesian Inference for the RSM

We now turn to the task of performing VB inference for the RSM signal model. The signal model employed by the RSM framework is shown in (13) and visualized in Fig. 1. In the following, let  $\mathbf{z} = (\{\mathbf{X}_{(:,i)}\}_{i=1}^L, \{\mathbf{E}_{(:,i)}\}_{i=1}^L, \{\boldsymbol{\gamma}_c\}_{c=1}^C, \{\mathbf{D}_{(j,i)}\}_{j=1, i=1}^{j=d, i=L})$  be the set of latent variables.

##### 3.2.1 Computation of $q(\mathbf{X}_{(:,i)})$

Using (17), we find that  $q(\mathbf{X}_{(:,i)}) = N(\mathbf{X}_{(:,i)}; \boldsymbol{\mu}^{\mathbf{x}}_{(:,i)}, \boldsymbol{\Sigma}^{\mathbf{x}})$ , where

$$\boldsymbol{\Sigma}^{\mathbf{x}} = \left( (\lambda)^{-1} \mathbf{A}^T \mathbf{A} + (\boldsymbol{\Gamma})^{-1} \right)^{-1} \quad (18)$$

$$\boldsymbol{\mu}^{\mathbf{x}}_{(:,i)} = (\lambda)^{-1} \boldsymbol{\Sigma}^{\mathbf{x}} \mathbf{A}^T (\mathbf{Y}_{(:,i)} - \langle \mathbf{E}_{(:,i)} \rangle) \quad (19)$$

and  $\boldsymbol{\Gamma}$  is a diagonal matrix with the  $(j, j)$ 'th entry given by  $\langle \frac{1}{\boldsymbol{\gamma}_c} \rangle$ , for  $j \in g_c$ . We use  $\langle \mathbf{z}_k \rangle$  to denote the expectation of the random variable  $\mathbf{z}_k$  with respect to  $q_k$ . Note that  $\{q(\mathbf{X}_{(:,i)})\}_{i=1}^L$  share the same covariance matrix  $\boldsymbol{\Sigma}^{\mathbf{x}}$ .

##### 3.2.2 Computation of $q(\mathbf{E}_{(:,i)})$

Using (17), we find that  $q(\mathbf{E}_{(:,i)}) = N(\mathbf{E}_{(:,i)}; \boldsymbol{\mu}^{\mathbf{e}}_{(:,i)}, \boldsymbol{\Sigma}^{\mathbf{e}}_i)$ , where

$$\boldsymbol{\Sigma}^{\mathbf{e}}_i = \left( (\lambda)^{-1} \mathbf{I} + \boldsymbol{\Delta}_i \right)^{-1} \quad (20)$$

$$\boldsymbol{\mu}^{\mathbf{e}}_{(:,i)} = (\lambda)^{-1} \boldsymbol{\Sigma}^{\mathbf{e}}_i (\mathbf{Y}_{(:,i)} - \mathbf{A} \langle \mathbf{X}_{(:,i)} \rangle) \quad (21)$$

and  $\boldsymbol{\Delta}_i$  is a diagonal matrix with the  $(j, j)$ 'th entry equal to  $\langle \frac{1}{\mathbf{D}_{(j,i)}} \rangle$ .

##### 3.2.3 Computation of $q(\boldsymbol{\gamma}_c)$ and $q(\mathbf{D}_{(j,i)})$

Using (17), we find that  $q(\boldsymbol{\gamma}_c) = IG\left(\boldsymbol{\gamma}_c; \frac{L|g_c|}{2} + \alpha_\gamma, \frac{\langle \|\mathbf{X}_{(g_c,:)}\|_F^2 \rangle}{2} + \beta_\gamma\right)$  and  $q(\mathbf{D}_{(j,i)}) = IG\left(\mathbf{D}_{(j,i)}; \frac{1}{2} + \alpha_\delta, \frac{\langle \mathbf{E}_{(j,i)}^2 \rangle}{2} + \beta_\delta\right)$ .

#### 3.3 Summary

It is evident from Sections 3.2.1-3.2.3 that all of the  $q_k$  depend on the moments of one or more latent variables. We will use an iterative procedure where we initialize the moments and, at each iteration, update the estimate of  $q_k$  based on the current estimates of  $\{q_{k'}\}_{k' \neq k}$ , repeating the process for all  $k$  until convergence. For clarity, we summarize the required moments for our iterative procedure:

$$\left\langle \frac{1}{\boldsymbol{\gamma}_c} \right\rangle = \frac{\frac{L|g_c|}{2} + \alpha_\gamma}{\frac{\langle \|\mathbf{X}_{(g_c,:)}\|_F^2 \rangle}{2} + \beta_\gamma} \quad (22)$$

$$\left\langle \frac{1}{\mathbf{D}_{(j,i)}} \right\rangle = \frac{\frac{1}{2} + \alpha_\delta}{\frac{\langle \mathbf{E}_{(j,i)}^2 \rangle}{2} + \beta_\delta} \quad (23)$$

$$\langle \mathbf{E}_{(:,i)} \rangle = \boldsymbol{\mu}^{\mathbf{e}}_{(:,i)}, \quad \langle \mathbf{X}_{(:,i)} \rangle = \boldsymbol{\mu}^{\mathbf{x}}_{(:,i)} \quad (24)$$

$$\langle \mathbf{E}_{(j,i)}^2 \rangle = \left( \boldsymbol{\mu}^{\mathbf{e}}_{(j,i)} \right)^2 + (\boldsymbol{\Sigma}^{\mathbf{e}}_i)_{(j,j)} \quad (25)$$

$$\langle \|\mathbf{X}_{(g_c,:)}\|_F^2 \rangle = \|\mathbf{M}_{(g_c,:)}\|_F^2 + L \times \text{trace} \left( \boldsymbol{\Sigma}^{\mathbf{x}}_{(g_c,:)} \right) \quad (26)$$

where  $\mathbf{M} = \begin{bmatrix} \boldsymbol{\mu}^{\mathbf{x}}_{(:,1)} & \dots & \boldsymbol{\mu}^{\mathbf{x}}_{(:,L)} \end{bmatrix}$ . Although it is possible to estimate  $\lambda$  within the Bayesian framework, we choose to select it using cross validation.

**Require:**  $\mathbf{Y}, \mathbf{A}, \{g_c\}_{c=1}^C, \lambda, T, \zeta, \tau$

- 1: Initialize  $\Omega = \{1, \dots, C\}, \boldsymbol{\gamma}_c = 1, \boldsymbol{\mu}_{(j,i)}^x = 1, \mathbf{D}_{(j,i)} = 1 \quad \forall c, j, i$
- 2: **for**  $r = 1$  to  $C$  **do**
- 3:   **for**  $t = 1$  to  $T$  **do**
- 4:      $\boldsymbol{\mu}^0 \leftarrow \boldsymbol{\mu}^x$
- 5:     Update parameters of  $q(\mathbf{X}_{(:,i)}), q(\boldsymbol{\gamma}_c), q(\mathbf{E}_{(:,i)}), q(\mathbf{D}_{(j,i)})$   
 $\forall c, j, i$
- 6:     Update moments in (22)-(26)
- 7:     **if**  $t == \zeta T$  **then**
- 8:       Save moments
- 9:     **end if**
- 10:   **end for**
- 11:   Compute  $\mathbf{r}_c^{SRID}$  using (6) for all  $c \in \Omega$
- 12:   Find  $c^* = \arg \min_c \mathbf{r}_c^{SRID}$ ,
- 13:   Set  $\boldsymbol{\psi}_r \leftarrow c^*$  and  $\Omega \leftarrow \Omega \setminus c^*$
- 14:   Remove columns of  $\mathbf{A}$  corresponding to  $c^*$
- 15:    $T \leftarrow \tau T$
- 16:   Re-initialize moments using saved values, removing any elements corresponding to  $c^*$
- 17: **end for**
- 18:
- 19: **return**

Fig. 2. RSM algorithm

The remaining design element of RSM is the choice of ranking strategy. Given a probe video, we begin by performing the VB inference procedure until convergence. We then use  $\boldsymbol{\mu}^x$  and  $\boldsymbol{\mu}^e$  as point estimates of  $\mathbf{X}$  and  $\mathbf{E}$ , respectively, compute residuals for each subject in the gallery using (6), and set  $\boldsymbol{\psi}_1$  to the subject which achieves the minimum residual. Next, we remove columns of  $\mathbf{A}$  corresponding to  $\boldsymbol{\psi}_1$  and repeat the process. The motivation for this strategy comes from [7], where Lisanti *et al.* argue that the coefficients in  $\mathbf{X}$  are dominated by a few subjects in the gallery. By removing the contribution of subject  $\boldsymbol{\psi}_r$  from  $\mathbf{A}$  and re-estimating  $\mathbf{X}$ , we hope that  $\boldsymbol{\psi}_{r+1}$  will be more accurate because  $\mathbf{X}$  will contain more information about subjects which *have not* been ranked yet.

Since re-estimating  $\mathbf{X}$  for  $C$  subjects can be computationally burdensome, we introduce a slight optimization shortcut. While performing inference for rank  $r$ , we save the state of the algorithm at  $\zeta T$  iterations, where  $T$  is the total number of iterations and  $0 < \zeta \leq 1$ . Then, we initialize the inference computations for rank  $r+1$  with the saved state and set  $T$  to  $\tau T$ , where  $0 < \tau \leq 1$ . The number of iterations needed to compute  $\boldsymbol{\psi}_r$  decays geometrically with increasing  $r$ , providing a considerable decrease in computational cost. At the same time, performance loss is mitigated by the "warm" initialization strategy. The complete algorithm is summarized in Alg. 2.

## 4 INTERPRETATION OF UPDATES

Consider the point estimate  $\boldsymbol{\mu}_{(:,i)}^x$  of  $\mathbf{X}_{(:,i)}$ , formed after the proposed VB procedure converges. Substituting (18) in (19), we get

$$\boldsymbol{\mu}_{(:,i)}^x = (\mathbf{A}^T \mathbf{A} + \lambda \boldsymbol{\Gamma})^{-1} \mathbf{A}^T (\mathbf{Y}_{(:,i)} - \boldsymbol{\mu}_{(:,i)}^e). \quad (27)$$

We see that (27) is actually the solution of a weighted ridge regression problem, i.e. least squares fitting with weighted  $\ell_2$  norm regularization over the coefficient vector:

$$\boldsymbol{\mu}_{(:,i)}^x = \arg \min_{\mathbf{X}_{(:,i)}} \|\mathbf{Y}_{(:,i)} - \boldsymbol{\mu}_{(:,i)}^e - \mathbf{A} \mathbf{X}_{(:,i)}\|_2^2 + \lambda \|\boldsymbol{\Gamma}^{\frac{1}{2}} \mathbf{X}_{(:,i)}\|_2^2 \quad (28)$$

where  $\boldsymbol{\Gamma}^{\frac{1}{2}}$  is a diagonal matrix whose  $(j, j)$ 'th entry is  $\left(\frac{1}{\boldsymbol{\gamma}_c}\right)^{\frac{1}{2}}$ , for  $j \in g_c$ . The least squares fitting is done after removing the outlier estimate  $\boldsymbol{\mu}_{(:,i)}^e$  from the observation  $\mathbf{Y}_{(:,i)}$ , which makes our approach very robust.

Hence, we can relate the RSM to ISR [7], which uses a reweighted  $\ell_1$  formulation, shown in (5), and reports state-of-the-art results for a number of re-id datasets. Our inference procedure can be interpreted as a robust reweighted  $\ell_2$  norm minimization algorithm, where the weights are computed in the hyperparameter space, known as Type II inference. In the SR literature, researchers have shown the superiority of Type II methods over methods which perform inference in the  $\mathbf{X}$  space, which are termed Type I and include ISR and SRID [31]. This observation motivated us to use a Type II based inference procedure for the re-id problem. As shown in Section 5, our Type II approach shows significant improvement over ISR and SRID, as well as other re-id algorithms not based on SR.

Another key advantage of RSM lies in its ability to capture the essence of multi-shot data. We can see from (28) that the weight matrix  $\boldsymbol{\Gamma}^{\frac{1}{2}}$  is shared among all  $L$  probe frames. The weighting scheme combines information from all  $L$  frames and takes advantage of the key fact that they belong to the same subject. Similarly, the moment computation for  $\frac{1}{\boldsymbol{\gamma}_c}$  in (22) combines information from all  $L$  frames.

## 5 RESULTS

In this section, we report experimental results on various re-id datasets. To highlight the capabilities of RSM, we focus on multi-shot re-id datasets, including ILIDS-VID [57], PRID 2011 [58], and CAVIAR4ReID [22]. In addition, we also present results for a single-shot re-id task on the VIPeR dataset [59] in order to show that RSM is competitive with other single-shot re-id algorithms. We report results in terms of the cumulative matching characteristic (CMC). In addition, we use  $\alpha_\gamma = \alpha_\delta = \beta_\gamma = \beta_\delta = 0$ .

### 5.1 Performance on ILIDS-VID

The ILIDS-VID dataset contains 300 subjects with sequences from two camera views, with 23 – 192 frames per subject per view. The dataset exhibits significant lighting, viewpoint, and occlusion variations and is ideal to showcase the capabilities of RSM. We elected to use the LOMO [13] feature space, which has been shown to produce state-of-the-art results on a number of re-id datasets. Because of the large amount of data available in ILIDS-VID, we also learned the XQDA [13] metric, which allowed us to reduce the dimensionality of the data to  $d = 100$ . We adopt the experimental procedure used in [3] and randomly split the dataset into training and test sets. The training set is used to learn the XQDA metric, which is then applied to project the test data. For a given train-test split, we randomly select  $L = 10$  frames per subject for the gallery and probe sets. This procedure is repeated 10 times for each train-test split and the train-test split is itself repeated 10 times (for a total of 100 experiments), and we report averaged results. We select  $\lambda = 10, \zeta = \tau = 0.5$  using

Classifier	Feature space	ILIDS-VID				PRID 2011			
		Rank 1	Rank 5	Rank 10	Rank 20	Rank 1	Rank 5	Rank 10	Rank 20
RSM	LOMO + XQDA [13]	<b>96.6</b>	<b>99.6</b>	<b>99.9</b>	<b>99.9</b>	<b>99.4</b>	<b>99.9</b>	<b>100</b>	<b>100</b>
ISR [7]	LOMO+ XQDA [13]	85.1	95.2	97.2	98.5	99.1	99.8	99.9	<b>100</b>
SRID [3]	Gray and Tao [8] + LFDA [9]	24.9	44.5	55.6	66.2	35.1	59.4	69.8	79.7
TAPR [52]	LOMO [52]	55	87.5	93.8	97.2	68.6	94.6	97.4	98.9
Softmax	Deep RNN [6]	58	84	91	96	70	90	95	97
NN	Deep CNN [5]	42.6	70.2	86.4	92.3	49.8	77.4	90.7	94.6
TDL [53]	HOG3D [16]	56.3	87.6	95.6	98.3	56.7	80	87.6	93.6
NN	Saliency [15]	10.2	24.8	35.5	52.9	25.8	43.6	52.6	62
RPRF [54]	Gray and Tao [8]	14.5	29.8	40.7	58.1	19.3	38.4	51.6	68.1
DVR [55]	HOD3D [16]	23.3	42.4	55.3	68.4	28.9	55.3	65.5	82.8
RankSVM [56]	Color & LBP [34]	23.2	44.2	54.1	68.8	34.3	56	65.5	77.3
NN	SDALF [10]	6.3	18.8	27.1	37.3	5.2	20.7	32	47.9

TABLE 1  
CMC results for ILIDS-VID and PRID2011 datasets.

Classifier	Feature space	Rank 1	Rank 5	Rank 10	Rank 20
RSM	WHOS [7]	<b>95.8</b>	<b>98.6</b>	<b>100</b>	<b>100</b>
ISR [7]	WHOS [7]	90.1	97.6	99	99.7
Bayes	CPS [18]	17.5	47.5	68	86
NN	SDALF [10]	8.3	37.5	58	77.5
Bayes	AHPE [19]	7.5	32	65	72

TABLE 2  
CMC results for CAVIAR4ReID dataset.

cross-validation. For comparison, we report the performance of ISR using LOMO+XQDA features on the ILIDS-VID dataset even though [7] did not consider this dataset nor this feature space.

The experimental results are shown in Table 1. The experimental setup for the SR based RSM, ISR, and SRID is identical. The remaining methods in Table 1 use  $L > 10$ . Since the amount of information about the probe increases with increasing  $L$ , we argue that Table 1 is not biased towards SR based methods and provides a fair comparison of competing methods. The results show that RSM outperforms all competing algorithms, including the SR based ISR and SRID methods as well as algorithms based on nearest neighbors (NN) [5], [10], [15], RankSVM [56], etc. Despite the serious challenges presented by the ILIDS-VID dataset, RSM is able to achieve 96.6% accuracy at rank 1, which is 38.6% higher (in absolute terms) than the best reported result in the literature and 11.5% higher than ISR. This shows that there is significant discriminative information in the multi-shot re-id problem and considerable performance gains can be achieved by algorithms which take advantage of this. Moreover, the results in Table 1 show that the LOMO+XQDA feature space is well-suited for difficult re-id problems, since ISR is able to outperform all of the algorithms reported in the literature (with the exception of the proposed RSM) by simply adopting this feature space.

## 5.2 Performance on PRID 2011

The PRID 2011 dataset contains 200 subjects with sequences from two camera views, with 5 – 675 frames per subject per view. Unlike ILIDS-VID, PRID 2011 does not contain occlusions and thus makes re-id significantly *easier*. As in the ILIDS-VID experiment, we use the LOMO feature space and learn a  $d = 100$  XQDA embedding after splitting the dataset into training and test sets. We adopt the setup in [3], [5], [53]. For each train-test split, we select  $L = 10$  frames per subject for the gallery and probe. This procedure is repeated 10 times for each train-test split and the train-test split is itself repeated 10 times (for a total of 100 experiments), and we report averaged results. We select  $\lambda = 10, \zeta = \tau = 0.5$  using cross-validation. As with ILIDS-VID, we report the performance of ISR using LOMO+XQDA features, despite the fact that [7] did not consider this dataset nor this feature space.

The experimental setup for the SR based RSM, ISR, and SRID is identical. The remaining methods use  $L > 10$ , which, as argued in Section 5.1, does not prevent us from conducting a fair comparison between the competing methods. The experimental results are shown in Table 1. The results show that RSM achieves 99.4% rank 1 accuracy on this dataset, which is a 29.4% improvement (in absolute terms) over the best published result. Interestingly, ISR achieves 99.1% rank 1 accuracy on this dataset, despite the fact that ISR *does not* model joint sparsity of  $\{\mathbf{X}_{(:,i)}\}_{i=1}^L$ . This suggests that the SR re-id framework paired with the LOMO+XQDA feature space is robust enough to tackle the PRID 2011 dataset.

## 5.3 Performance on CAVIAR4ReID

To show the performance of RSM independently of the LOMO+XQDA feature space and to better compare RSM with ISR [7], we evaluate the performance of RSM on the CAVIAR4ReID dataset using the WHOS<sup>1</sup> feature space [7]. This dataset contains 72 subjects, with sequences collected from one or two camera views. Each sequence contains 10 frames, with the frames exhibiting significant resolution, lighting, and occlusion variation. In this instance,  $d = 2960$  and  $N = 360$ .

We follow the experimental setup in [7] and randomly split the dataset into gallery and probe sets, with each set containing  $L = 5$  frames per subject. We repeat this process 50 times and report averaged results. We select  $\lambda = 1e-4, \zeta = \tau = 0.5$  using cross-validation. The experimental results are reported in Table 2<sup>2</sup>. The experimental conditions for all of the methods reported are identical. The results show that RSM consistently outperforms ISR for all ranks, with the largest performance gap at rank 1 where RSM outperforms ISR by 5.7% (absolute). Both RSM and ISR outperform approaches reported in the literature by a large margin.

## 5.4 Performance on VIPeR

Finally, we report results for the VIPeR dataset, which is a single-shot re-id dataset containing 300 subjects recorded from two views. To compare with ISR, we employ the WHOS feature space. Following [7], we randomly select  $L = 1$  frame per subject for the gallery and probe, repeating the procedure 10 times. Table 3 shows the rank 1 accuracy results. The results show that RSM is competitive with state-of-the-art single-shot algorithms, even though RSM was primarily designed to tackle multi-shot problems.

1. Made available by the authors of [7] at <http://www.micc.unifi.it/lisanti/source-code/whos/>.

2. We do not report results for SRID because this dataset was not considered in [3] and the implementation is not publicly available.

Classifier	Feature space	Rank 1
RSM	WHOS [7]	26.4
ISR [7]	WHOS [7]	<b>27</b>
NN	SDALF [10]	19.9
Bayes	CPS [18]	21.8
RPLM [34]	HSV + LAB + LBP	<b>27</b>
EIML [17]	HSV + LAB + LBP	22
eSCD [15]	LAB + SIFT	26.7

TABLE 3  
Rank 1 accuracy (%) on VIPeR dataset.

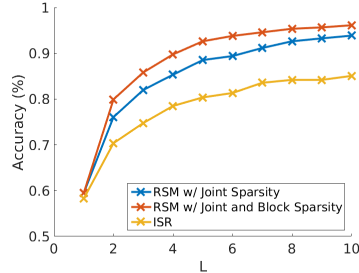


Fig. 3. ILIDS-VID rank 1 accuracy as a function of  $L$ .

## 5.5 Why RSM?

We now turn to the question of why RSM outperforms competing algorithms on the re-id problem. To motivate our arguments, we conduct a re-id experiment on the ILIDS-VID dataset using the LOMO+QXDA feature space and test the rank 1 accuracy of RSM and ISR as a function of the number  $L$  of gallery and probe frames per subject. To assess the influence of the various components of the RSM model on re-id performance, we show results for RSM with the joint and block sparsity components (i.e. the model detailed in Section 2.2) as well as with the joint sparsity component but not the block sparsity component. The results are shown in Fig. 3. First, we observe that even at  $L = 1$ , RSM outperforms ISR by 1.2% (in absolute terms). This provides evidence for the claim made in Section 4 that the Type II inference procedure employed by RSM is superior to the Type I inference performed by ISR. Second, we see that there is an appreciable improvement in performance between RSM with joint sparsity and RSM with both joint and block sparsity. This suggests that each component of the RSM model provides a tangible improvement in re-id accuracy. Finally, the results show that the rank 1 accuracy of RSM increases with increasing  $L$ , consistently outperforming ISR. In fact, the performance gap between RSM with joint and block sparsity and ISR *increases* from  $L = 1$  to  $L = 6$ , confirming the claim that RSM is *better* able to harness the increasing amount of information about the probe subject as  $L$  increases.

## 6 CONCLUSION

In this work, we presented the RSM re-id algorithm, which, to the best of our knowledge, is the first Bayesian SR based re-id algorithm. The RSM is capable of modeling all of the relevant aspects of the multi-shot re-id problem, including the block structure of the gallery  $\mathbf{A}$ , joint sparsity of the probe frames  $\{\mathbf{X}_{(:,i)}\}_{i=1}^L$ , and sparse observation noise introduced by occlusions, viewpoint variations, and illuminated changes. In addition we introduced an efficient VB inference procedure and ranking scheme. We showed that RSM achieves state-of-the-art CMC results on every multi-shot re-id dataset considered and is competitive with existing approaches on the single-shot problem.

## REFERENCES

- [1] I. O. De Oliveira and J. L. de Souza Pio, "People reidentification in a camera network," in *Dependable, Autonomic and Secure Computing, 2009. DASC '09. Eighth IEEE International Conference on*. IEEE, 2009, pp. 461–466.
- [2] S. Gong, M. Cristani, S. Yan, and C. C. Loy, *Person re-identification*. Springer, 2014, vol. 1.
- [3] S. Karanam, Y. Li, and R. J. Radke, "Sparse re-id: Block sparsity for person re-identification," in *Proceedings of the IEEE Conference on Computer Vision and Pattern Recognition Workshops*, 2015, pp. 33–40.
- [4] O. Hamdoun, F. Moutarde, B. Stanculescu, and B. Steux, "Person re-identification in multi-camera system by signature based on interest point descriptors collected on short video sequences," in *Distributed Smart Cameras, 2008. ICDS-C 2008. Second ACM/IEEE International Conference on*. IEEE, 2008, pp. 1–6.
- [5] L. Wu, C. Shen, and A. v. d. Hengel, "Deep recurrent convolutional networks for video-based person re-identification: An end-to-end approach," *arXiv preprint arXiv:1606.01609*, 2016.
- [6] N. McLaughlin, J. Martinez del Rincon, and P. Miller, "Recurrent convolutional network for video-based person re-identification," in *Proceedings of the IEEE Conference on Computer Vision and Pattern Recognition*, 2016, pp. 1325–1334.
- [7] G. Lisanti, I. Masi, A. D. Bagdanov, and A. Del Bimbo, "Person re-identification by iterative re-weighted sparse ranking," *IEEE transactions on pattern analysis and machine intelligence*, vol. 37, no. 8, pp. 1629–1642, 2015.
- [8] D. Gray and H. Tao, "Viewpoint invariant pedestrian recognition with an ensemble of localized features," in *European conference on computer vision*. Springer, 2008, pp. 262–275.
- [9] X. Niyogi, "Locality preserving projections," in *Neural information processing systems*, vol. 16. MIT, 2004, p. 153.
- [10] M. Farenzena, L. Bazzani, A. Perina, V. Murino, and M. Cristani, "Person re-identification by symmetry-driven accumulation of local features," in *Computer Vision and Pattern Recognition (CVPR), 2010 IEEE Conference on*. IEEE, 2010, pp. 2360–2367.
- [11] O. Tuzel, F. Porikli, and P. Meer, "Region covariance: A fast descriptor for detection and classification," in *European conference on computer vision*. Springer, 2006, pp. 589–600.
- [12] S. Bak, E. Corvee, F. Bremond, and M. Thonnat, "Multiple-shot human re-identification by mean riemannian covariance grid," in *Advanced Video and Signal-Based Surveillance (AVSS), 2011 8th IEEE International Conference on*. IEEE, 2011, pp. 179–184.
- [13] S. Liao, Y. Hu, X. Zhu, and S. Z. Li, "Person re-identification by local maximal occurrence representation and metric learning," in *Proceedings of the IEEE Conference on Computer Vision and Pattern Recognition*, 2015, pp. 2197–2206.
- [14] E. Corvee, F. Bremond, M. Thonnat *et al.*, "Person re-identification using spatial covariance regions of human body parts," in *Advanced Video and Signal Based Surveillance (AVSS), 2010 Seventh IEEE International Conference on*. IEEE, 2010, pp. 435–440.
- [15] R. Zhao, W. Ouyang, and X. Wang, "Unsupervised saliency learning for person re-identification," in *Proceedings of the IEEE Conference on Computer Vision and Pattern Recognition*, 2013, pp. 3586–3593.
- [16] A. Klaser, M. Marszałek, and C. Schmid, "A spatio-temporal descriptor based on 3d-gradients," in *BMVC 2008-19th British Machine Vision Conference*. British Machine Vision Association, 2008, pp. 275–1.
- [17] M. Hirzer, P. M. Roth, and H. Bischof, "Person re-identification by efficient impostor-based metric learning," in *Advanced Video and Signal-Based Surveillance (AVSS), 2012 IEEE Ninth International Conference on*. IEEE, 2012, pp. 203–208.
- [18] D. S. Cheng, M. Cristani, M. Stoppa, L. Bazzani, and V. Murino, "Custom pictorial structures for re-identification," in *BMVC*, vol. 1, no. 2, 2011, p. 6.
- [19] L. Bazzani, M. Cristani, A. Perina, and V. Murino, "Multiple-shot person re-identification by chromatic and epitomic analyses," *Pattern Recognition Letters*, vol. 33, no. 7, pp. 898–903, 2012.
- [20] J. Wright, A. Y. Yang, A. Ganesh, S. S. Sastry, and Y. Ma, "Robust face recognition via sparse representation," *Pattern Analysis and Machine Intelligence, IEEE Transactions on*, vol. 31, no. 2, pp. 210–227, 2009.
- [21] J. Wright, A. Ganesh, A. Yang, Z. Zhou, and Y. Ma, "Sparsity and robustness in face recognition," *arXiv preprint arXiv:1111.1014*, 2011.
- [22] D. S. Cheng, M. Cristani, M. Stoppa, L. Bazzani, and V. Murino, "Custom pictorial structures for re-identification," in *British Machine Vision Conference (BMVC)*, 2011.
- [23] E. Elhamifar and R. Vidal, "Sparse subspace clustering," in *Computer Vision and Pattern Recognition, 2009. CVPR 2009. IEEE Conference on*. IEEE, 2009, pp. 2790–2797.

- [24] M. T. Harandi, C. Sanderson, R. Hartley, and B. C. Lovell, "Sparse coding and dictionary learning for symmetric positive definite matrices: A kernel approach," in *Computer Vision—ECCV 2012*. Springer, 2012, pp. 216–229.
- [25] M. Elad, *Sparse and Redundant Representations*. Springer New York, 2010.
- [26] R. G. Baraniuk, "Compressive sensing," *IEEE signal processing magazine*, vol. 24, no. 4, 2007.
- [27] Y. C. Eldar, P. Kuppinger, and H. Bölcskei, "Block-sparse signals: Uncertainty relations and efficient recovery," *Signal Processing, IEEE Transactions on*, vol. 58, no. 6, pp. 3042–3054, 2010.
- [28] Z. Zhang and B. D. Rao, "Extension of sbl algorithms for the recovery of block sparse signals with intra-block correlation," *IEEE Transactions on Signal Processing*, vol. 61, no. 8, pp. 2009–2015, 2013.
- [29] D. P. Wipf and B. D. Rao, "An empirical bayesian strategy for solving the simultaneous sparse approximation problem," *Signal Processing, IEEE Transactions on*, vol. 55, no. 7, pp. 3704–3716, 2007.
- [30] M. E. Tipping, "Sparse bayesian learning and the relevance vector machine," *The journal of machine learning research*, vol. 1, pp. 211–244, 2001.
- [31] R. Giri and B. Rao, "Type i and type ii bayesian methods for sparse signal recovery using scale mixtures," *IEEE Transactions on Signal Processing*, vol. 64, no. 13, pp. 3418–3428, July 2016.
- [32] I. Fedorov, R. Giri, B. D. Rao, and T. Q. Nguyen, "Robust bayesian method for simultaneous block sparse signal recovery with applications to face recognition," in *2016 IEEE International Conference on Image Processing (ICIP)*, Sept 2016, pp. 3872–3876.
- [33] S. Karanam, M. Gou, Z. Wu, A. Rates-Borras, O. Camps, and R. J. Radke, "A comprehensive evaluation and benchmark for person re-identification: Features, metrics, and datasets," *arXiv preprint arXiv:1605.09653*, 2016.
- [34] M. Hirzer, P. M. Roth, M. Köstinger, and H. Bischof, "Relaxed pairwise learned metric for person re-identification," in *European Conference on Computer Vision*. Springer, 2012, pp. 780–793.
- [35] K. Q. Weinberger, J. Blitzer, and L. K. Saul, "Distance metric learning for large margin nearest neighbor classification," in *Advances in neural information processing systems*, 2005, pp. 1473–1480.
- [36] M. Sugiyama, "Local fisher discriminant analysis for supervised dimensionality reduction," in *Proceedings of the 23rd international conference on Machine learning*. ACM, 2006, pp. 905–912.
- [37] M. I. Khedher, M. A. El Yacoubi, and B. Dorizzi, "Multi-shot surf-based person re-identification via sparse representation," in *Advanced Video and Signal Based Surveillance (AVSS), 2013 10th IEEE International Conference on*. IEEE, 2013, pp. 159–164.
- [38] E. J. Candes, M. B. Wakin, and S. P. Boyd, "Enhancing sparsity by reweighted  $l_1$  minimization," *Journal of Fourier analysis and applications*, vol. 14, no. 5-6, pp. 877–905, 2008.
- [39] D. P. Wipf and B. D. Rao, "Sparse bayesian learning for basis selection," *Signal Processing, IEEE Transactions on*, vol. 52, no. 8, pp. 2153–2164, 2004.
- [40] D. F. Andrews and C. L. Mallows, "Scale mixtures of normal distributions," *Journal of the Royal Statistical Society. Series B (Methodological)*, pp. 99–102, 1974.
- [41] J. A. Palmer, "Variational and scale mixture representations of non-gaussian densities for estimation in the bayesian linear model: Sparse coding, independent component analysis, and minimum entropy segmentation," 2006.
- [42] J. Palmer, K. Kreutz-Delgado, B. D. Rao, and D. P. Wipf, "Variational em algorithms for non-gaussian latent variable models," in *Advances in neural information processing systems*, 2005, pp. 1059–1066.
- [43] K. Lange and J. S. Sinsheimer, "Normal/independent distributions and their applications in robust regression," *Journal of Computational and Graphical Statistics*, vol. 2, no. 2, pp. 175–198, 1993.
- [44] A. P. Dempster, N. M. Laird, and D. B. Rubin, "Iteratively reweighted least squares for linear regression when errors are normal/independent distributed," 1980.
- [45] —, "Maximum likelihood from incomplete data via the em algorithm," *Journal of the royal statistical society. Series B (methodological)*, pp. 1–38, 1977.
- [46] Z. Zhang and B. D. Rao, "Sparse signal recovery with temporally correlated source vectors using sparse bayesian learning," *Selected Topics in Signal Processing, IEEE Journal of*, vol. 5, no. 5, pp. 912–926, 2011.
- [47] T. Li and Z. Zhang, "Robust face recognition via block sparse bayesian learning," *Mathematical Problems in Engineering*, vol. 2013, 2013.
- [48] D. J. MacKay, "Ensemble learning and evidence maximization," in *Proc. Nips*, vol. 10, no. 1.54. Citeseer, 1995, p. 4083.
- [49] M. I. Jordan, Z. Ghahramani, T. S. Jaakkola, and L. K. Saul, "An introduction to variational methods for graphical models," *Machine learning*, vol. 37, no. 2, pp. 183–233, 1999.
- [50] C. M. Bishop, "Pattern recognition," *Machine Learning*, vol. 128, 2006.
- [51] S. Boyd and L. Vandenberghe, *Convex optimization*. Cambridge university press, 2004.
- [52] C. Gao, J. Wang, L. Liu, J.-G. Yu, and N. Sang, "Temporally aligned pooling representation for video-based person re-identification," in *Image Processing (ICIP), 2016 IEEE International Conference on*. IEEE, 2016, pp. 4284–4288.
- [53] J. You, A. Wu, X. Li, and W.-S. Zheng, "Top-push video-based person re-identification," *arXiv preprint arXiv:1604.08683*, 2016.
- [54] Y. Li, Z. Wu, and R. J. Radke, "Multi-shot re-identification with random-projection-based random forests," in *2015 IEEE Winter Conference on Applications of Computer Vision*. IEEE, 2015, pp. 373–380.
- [55] T. Wang, S. Gong, X. Zhu, and S. Wang, "Person re-identification by video ranking," in *European Conference on Computer Vision*. Springer, 2014, pp. 688–703.
- [56] O. Chapelle and S. S. Keerthi, "Efficient algorithms for ranking with svms," *Information Retrieval*, vol. 13, no. 3, pp. 201–215, 2010.
- [57] T. Wang, S. Gong, X. Zhu, and S. Wang, "Person re-identification by discriminative selection in video ranking," 2016.
- [58] M. Hirzer, C. Beleznai, P. M. Roth, and H. Bischof, "Person re-identification by descriptive and discriminative classification," in *Scandinavian conference on Image analysis*. Springer, 2011, pp. 91–102.
- [59] D. Gray, S. Brennan, and H. Tao, "Evaluating appearance models for recognition, reacquisition, and tracking," in *Proc. IEEE International Workshop on Performance Evaluation for Tracking and Surveillance (PETS)*, vol. 3, no. 5. Citeseer, 2007.



**Igor Fedorov** (S'15) received the B.S and M.S. degrees in Electrical Engineering from the University of Illinois at Urbana-Champaign in 2012 and 2014, respectively. He is currently pursuing a Ph.D. degree in Electrical Engineering at the University of California, San-Diego. His research interests include sparse signal recovery, machine learning, and signal processing.



**Ritwik Giri** (S'13) received B.E. degree in Electronics and Telecommunication Engineering from Jadavpur University, India in 2011. He also received M.S. and Ph.D. degrees in electrical engineering from the University of California, San Diego, La Jolla, CA, USA, in 2014 and 2016 respectively. He is currently working as a DSP Research Engineer at Starkey Hearing Technologies, Eden Prairie, MN, USA.



**Bhaskar D. Rao** (S'80-M'83-SM'91-F'00) received the B.Tech. degree in electronics and electrical communication engineering from the Indian Institute of Technology, Kharagpur, India, and the M.S. and Ph.D. degrees in electrical engineering from the University of Southern California, Los Angeles, Los Angeles, CA, USA, in 1979, 1981, and 1983, respectively. Since 1983, he has been with the University of California San Diego, La Jolla, CA, USA, where he is currently a Professor with the Department of Electrical and Computer Engineering and holds the Ericsson Endowed Chair in wireless access networks. He was the Director of the Center for Wireless Communications from 2008 to 2011.



**Truong Q. Nguyen** (F05) received the B.S., M.S., and Ph.D. degrees from California Institute of Technology, Pasadena, CA, USA, in 1985, 1986, and 1989, respectively. He is a Professor with the Electrical and Computer Engineering Department, University of California at San Diego, San Diego, CA, USA. He has co-authored a textbook entitled *Wavelets and Filter Banks* (Wellesley-Cambridge, 1997; with Prof. G. Strang), and authored several MATLAB-based toolboxes in image compression, electro-

cardiogram compression, and filter bank design. He has also authored over 400 publications.